MAGNETIC MICROSTRUCTURE OF THIN FILMS AND SURFACES: EXPLOITING SPIN-POLARIZED ELECTRONS IN THE SEM AND STM

D.T. PIERCE, M.R. SCHEINFEIN, J. UNGURIS AND R.J. CELOTTA
National Institute of Standards and Technology, Gaithersburg, MD. 20899

ABSTRACT

Magnetic microstructure, that is the configuration of domains and domain walls in a magnetic material, is of both fundamental interest and of crucial importance for device applications. For example, the ultimate density of magnetic information storage is limited by the sharpness of a domain boundary. The magnetic microstructure of a thin film or surface depends sensitively on its physical structure which is strongly affected by sample preparation or growth. High resolution magnetization imaging is necessary to determine the domain configuration that occurs for a particular sample preparation and the changes that take place under external perturbations such as applied magnetic field, stress or temperature.

INTRODUCTION

Scanning Electron Microscopy with Polarization Analysis (SEMPA), in which the spin polarization of the secondary electrons is measured, is unique in domain imaging techniques using electron microscopy in that the image is directly proportional to the magnetization. In this sense it is like the magneto-optic Kerr effect without the spatial resolution of the technique being limited by optical wavelengths. Our ultimate goal of imaging spin configurations with atomic resolution may only be possible if scanning tunneling microscopy (STM) can be extended to include sensitivity to spin. Right now, the STM can be used to investigate the growth of magnetic films at the atomic level. In this article results of SEMPA studies of thin films and surfaces are possible. The further possibility of obtaining magnetic images with the STM is also discussed.

Advances in the growth of ultrathin magnetic films and multilayers suggest the possibility of atomically engineering materials to achieve special properties. Among the many magnetic properties that may differ between thin layers and those of the bulk are 1) the temperature dependence of the magnetization, both at low temperature and in the critical region (the Curie temperature itself may be different), 2) the anisotropy, to which there is a large shape dependent contribution and possibly also a significant surface contribution, 3) the size of the magnetic moments and spatial dependence of the magnetic order, 4) the magnetization processes, and 5) the magnetic microstructure. By magnetic microstructure we mean the details of the magnetization orientation in the domains and domain walls which form to lower the free energy of a ferromagnetic specimen. In this paper we focus on the magnetic microstructure, how we measure it and understand it, and show with some examples how these results are important from both a fundamental physics point of view and also for applications in magnetic technology.

MAGNETIC MICROSTRUCTURE

The main contributions to the magnetic free energy come from the magnetostatic energy, the anisotropy energy, and the exchange energy. Although the micromagnetic problem can be formulated, the actual domain configuration which is formed to minimize the energy can only be calculated

Mat. Res. Soc. Symp. Proc. Vol. 151. ©1989 Materials Research Society

for simple geometries and ideal materials. To investigate magnetic microstructure and how it affects macroscopic properties, it is necessary in practice to observe the domain configurations. Domains have long been observed using the Bitter method, in which fine metal particles collect on the surface of a ferromagnet in the field gradients at domain walls. Higher resolution observation of domains is possible with transmission Lorentz microscopy in which the deflection of the electron beam by the magnetic field provides domain contrast. Ideally one wants to measure a quantity directly related to the magnetization rather than to the field. This is possible with the magneto-optic Kerr effect,extending the range to include at higher spatial resolution, with scanning electron microscopy with polarization analysis(SEMPA). We will describe the principle of SEMPA for obtaining high resolution magnetization images and show results pertaining to edge acuity in a thin film recording media, thickness dependence of domain structure in permalloy thin film memory elements, existence of domains in few monolayer films, and the distribution of magnetization inside a domain wall. The outlook for achieving yet higher spatial resolution using scanned tip microscopy will be discussed.

The development of electron microscopy has been key to our knowledge of microstructure from biological specimens to metallurgical ones. By exploiting the information in the degree of electron spin polarization, we obtain information on magnetic properties of a specimen. In a 3d ferromagnet such as Fe, Co, or Ni, the magnetization M is directly proportional to the net spin density, $n^{\uparrow}-n_{\downarrow}$

$$M=-\mu_B(n_{\uparrow}-n_{\downarrow}) \qquad (1)$$

where $n_{\uparrow}(n_{\downarrow})$ the number of spins per unit volume parallel (antiparallel) to a particular direction. Spin polarized electron spectroscopies (photoemission, Auger, secondary electron) depend on extracting electrons from the solid without loss of information. One then measures the degree of spin polarization P, for example the z component, of the extracted beam,

$$P_z=(N_{\uparrow}-N_{\downarrow})/(N_{\uparrow}+N_{\downarrow}) \qquad (2)$$

where $N_{\uparrow}(N_{\downarrow})$ are the number of electrons with spins parallel (antiparallel) to the z direction. Low energy secondary electrons are primarily the result of electron-hole pair creation and thus reflect the net spin density of the valence band. The secondary electron spin polarization can be estimated as $P=n_B/n$, where n_B is the magnetic moment per atom and n is the number of valence electrons per atom; one estimates P to be 28%, 19%, and 5% for Fe, Co, and Ni respectively.

The measurement of magnetic microstructure by measuring the spin polarization of secondary electrons is illustrated in Fig. 1. A finely focused electron beam is rastered across the specimen and generates secondary electrons. A measurement of the secondary electron intensity gives the familiar SEM image of the topography. If additionally the spin polarization is measured, one obtains an image of the magnetization. All three components of the magnetization can be measured to obtain a complete vector image. A new type of spin analyzer, which is exceptionally compact and efficient, has been developed for this purpose. The experimental details of the SEMPA technique are described elsewhere [1-2].

A SEMPA magnetization image of a test magnetic pattern written on a disk is shown in Fig. 2a. In this case the active material is a 70 nm thick layer of Co-Ni (approximately 80%-20%). The image displays one component of the magnetization nearly aligned along the domains. A slight offset in the writing of successive tracks resulted from an alignment error as the recording head moved radially out on the disk. These domains are about 2 micrometers wide. In practice, the information is associated with the transition from one domain to another. For example a "1" could be

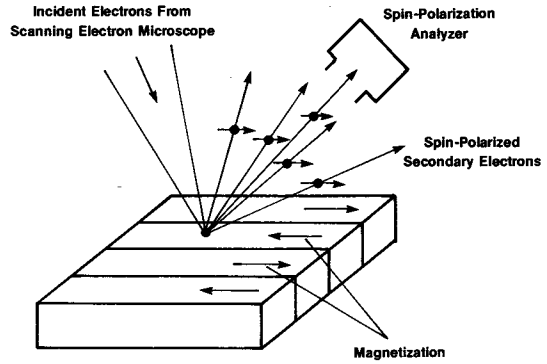

Fig. 1. A schematic illustration of the Scanning Electron Microscopy with Polarization Analysis (SEMPA) technique.

associated with a transition and a "0" with no transition. A sharp well defined boundary is desirable for the minimum noise signal. A region of Fig. 2a at ten times higher magnification is shown in Fig. 2b. At this magnification the jaggedness of the domain boundary is very evident. Clearly this puts a limitation on the recording density. The availability of SEMPA as a means to observe submicron scale magnetic microstructure can assist research efforts in recording media and the recording process to progress toward greater storage density.

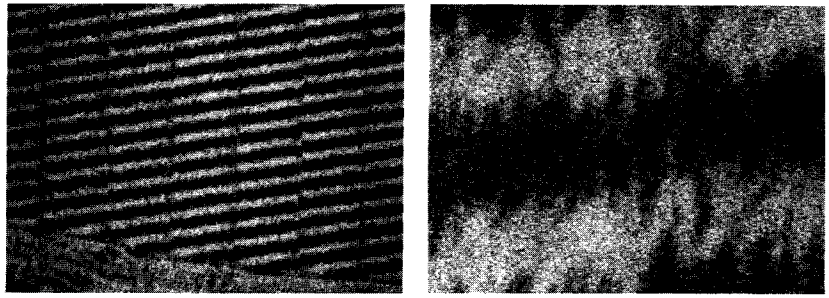

Fig. 2. Written bits in a Co-Ni recording media shown in (a) a low magnification, image 70 micrometers across, and in (b) at 10 times higher magnification.

Magnetic storage has the advantages of being nonvolatile and radiation resistant. Experimental random access memories have been tested using an array of permalloy elements which are etched into arrowhead shapes. The images of the horizontal and vertical components of the magnetization are shown in Fig. 3a and b respectively. The y-shaped domain shown in Fig. 3 is one of the two binary states. Since white represents magnetization pointing to the right and up in Fig. 3 a and b respectively, one can see that the magnetization vector rotates in a counter clockwise sense in the two elements on the left and in a clockwise sense in the two elements on

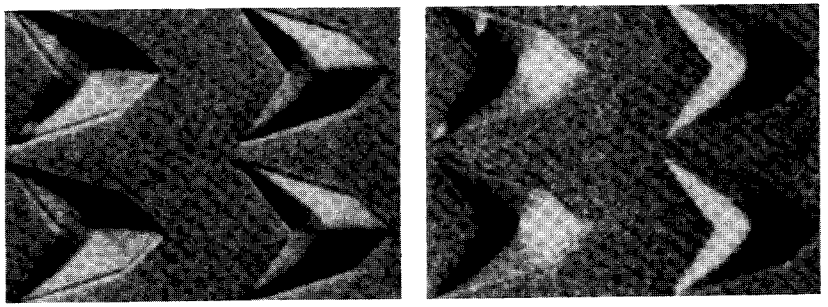

Fig. 3. SEMPA images of the (a) horizontal component and (b) vertical component of the magnetization on an array of permalloy memory elements. The images are 35 micrometers across.

the right of the figure. The magnetic state shown here represents a "1" in a memory device whereas the absence of a y-domain would represent a "0". The difference in the magnetoresistance of these two states provides the readout. One of the major advantages of magnetic imaging with SEMPA is that both in-plane magnetization components are measured simultaneously. This allows one to readily determine the rotation of the magnetization vector as just described, and in other cases to identify closure domains, edge curling, and domain walls.

The performance of magnetic memory devices depends sensitively on their shape, which influences the resultant magnetization configuration. The performance also depends on materials processing parameters such as evaporation rate, substrate temperature, and applied magnetic field during evaporation [3]. In developing such devices, the ability to observe the Y-domain configuration and its change as different geometrical and processing parameters are varied is essential. The dependence of the domains on thickness is illustrated in Fig. 4a which is a low magnification image 200 micrometers across. The elements in the left of the image are nominally 40 nm thick. Moving towards the right, the elements have been sputtered with the edge of a stationary 1keV Ar ion beam such that the permalloy thickness decreases progressively towards zero. This is seen clearly in Fig. 4b which shows a scanning Auger spectroscopy image of the Ni signal. The left most two columns of elements in Fig. 4a show the characteristic y-domain configuration. The central region of the figure shows that the domain patterns change with the decreasing thickness long before the reduced thickness is apparent in the Auger image.

An interesting question is how thin a magnetic film can be and still have magnetic domains. Some theories suggest that a monolayer film must be uniformly magnetized, that is have a single domain. However, recently Yafet and Gyorgy [4] have shown that for sufficiently large perpendicular surface anisotropy, K_s, domains form in a monolayer of ferromagnetically coupled spins. The difference in energy between the domain configuration and the uniformly magnetized configuration is small. Further theoretical work is in progress to predict below what temperature the domain configuration should be stable.

Experimentally, we have investigated [5] domains in ultrathin Fe films grown epitaxially by evaporation at room temperature on a Ag(100) surface. Figure 5 is an image of one component of the magnetization of a room temperature Fe film with an average thickness of 3.4 ML. The light region and dark region represent two oppositely magnetized domains. The difference in the degree of spin polarization of the secondary electrons

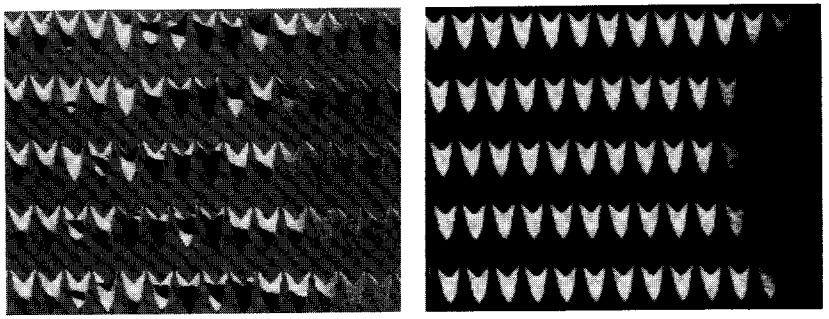

Fig. 4.(a) SEMPA and (b) Scanning Auger images of an array of experimental y-domain permalloy memory elements 200 micrometers across. The permalloy thickness varies from 40 nm at the left to zero at the right.

Fig. 5. SEMPA image of one component of the magnetization shows domains in a 3.4 monolayer average thickness Fe film evaporated on Ag(100).

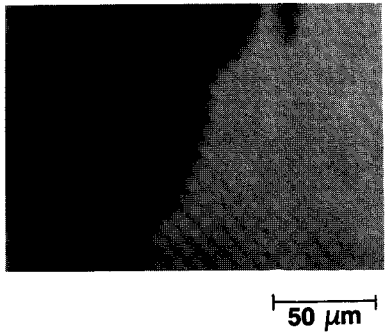

from the two domains is about 40%. This image is from an area approximately 150x200 micrometers. Most of the film consisted of a single domain except for a strip approximately 1 mm wide along the edge of the film where multidomain structures such as that displayed in Fig. 5 were observed. We did not observe domains in the same region for films 2.6 ML or less in thickness.

Further experimental work is planned to determine if domains are stable in a monolayer film. Clearly it is necessary to go to low temperature. However, there is a further critical problem to be overcome which is often overlooked in investigations which glibly speak of a single monolayer. How can a single monolayer film be prepared and how can it be verified that it has indeed been achieved? The magnetic properties of a uniform single layer may be quite different from the properties of a film consisting of epitaxial clusters such that the average thickness is one monolayer. Few substrates are smooth on an atomic scale and steps or defects could influence the magnetic properties. There is an immense amount of work to be done before we can speak confidently about and measure reproducibly the properties of a monolayer film.

Our discussion of magnetic microstructure so far has focused on the domains. Another aspect of magnetic microstructure is the internal structure of a domain wall, that is, how does the magnetization vary within the wall. In a 180 degree Bloch wall found inside a bulk ferromagnet, the magnetization rotates in the plane of the wall. Inside a thin film, with a typical thickness of a few tens of nanometers, it is energetically favorable for the magnetization to rotate in the plane of the film in order to avoid the poles which would be created if a Bloch wall intersected a surface. At intermediate thicknesses, "asymmetric" Bloch walls are known to occur [6]. For example, a view of the magnetization in the plane of a cross section through Fe films 0.1 and 0.5 micrometer thick are shown in

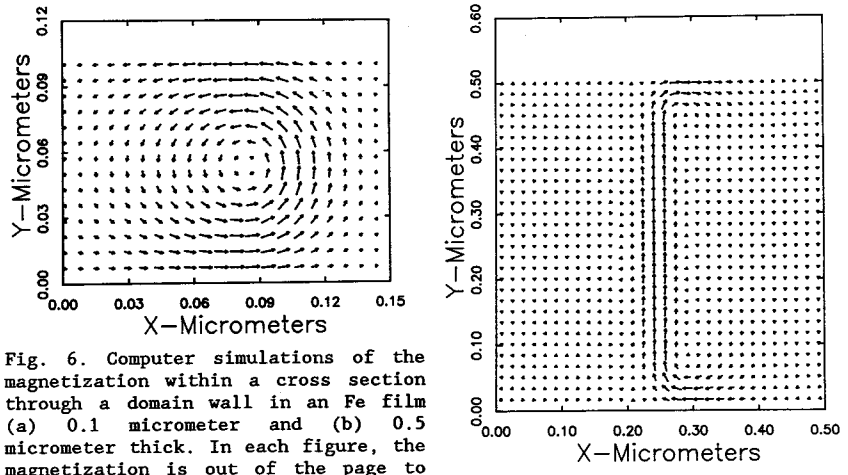

Fig. 6. Computer simulations of the magnetization within a cross section through a domain wall in an Fe film (a) 0.1 micrometer and (b) 0.5 micrometer thick. In each figure, the magnetization is out of the page to the left of the wall and into the page to the right of the wall.

Fig. 6 a and b respectively. In the thinner film, the vortex structure characteristic of an asymmetric Bloch wall in the interior is clearly apparent with Néel walls at the surface. In the thicker film, there is a well defined Bloch wall in the interior, again with Néel walls at the surface.

The magnetization distributions of Fig. 6 are the result of computer calculations in which the direction of the magnetization is varied to minimize the total magnetic energy. The calculated profiles of the surface Néel walls agree quantitatively with the profiles measured for an Fe single crystal, a Co based ferromagnetic glass, and a permalloy film [7]. A wide range of materials parameters, such as the anisotropy, K, the exchange constant, A, and the saturation magnetization, M_s, is covered by these three materials. For example, the anisotropy varies two orders of magnitude in going from Fe to permalloy. The presence of a Néel wall at the surface is a widespread phenomenon which occurs when the anisotropy energy near the surface is less than the magnetostatic energy, $K<2\pi M_s^2$. A film is thick enough to have a well defined Bloch wall when the thickness is typically several times $\sqrt{A/K}$. The thickness of the Bloch wall in the interior is less than half the thickness of the surface Néel wall.

In the extreme case of the monolayer film, the situation is different still. For a film magnetized in plane, a uniformly magnetized single domain with no domain walls is expected. However, if the perpendicular surface anisotropy is sufficiently large to cause domain formation, the domain wall is predicted to be a Bloch wall roughly 100 lattice constants wide [4]. Experimental tests of these predictions will be possible with the next generation of SEMPA systems assuming the materials problems inherent in producing uniform monolayer films can be overcome.

The asymmetric surface Néel wall which can be most clearly seen in the calculated magnetization distribution shown in Fig. 6b has a degeneracy in that it could bend over to the left instead of to the right as shown. As can be seen in Fig. 6b, the surface Néel wall is offset to the right from the interior Bloch wall. A surface Néel wall with opposite sense would be offset to the left. This can be seen experimentally in the SEMPA image of Fig. 7 showing the horizontal component of magnetization in a ferromagnetic glass (Allied 2705M, $Co_{69}Fe_4Ni_1Mo_2B_{12}Si_{12}$). The centers of the white and black surface Néel walls are displaced from each other as expected from

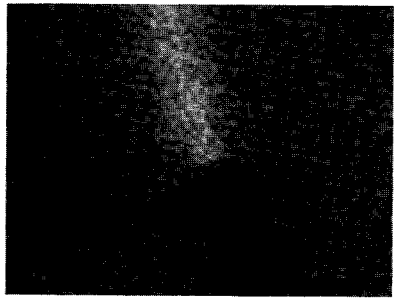

Fig. 7. SEMPA image of the horizontal component of the magnetization in a Co-based ferromagnetic glass shows the offset of two surface Néel walls. The magnetization running across the Néel walls changes sense at a point where a Bloch line intersects the surface.

Fig. 6b. The magnetization in the white wall is towards the right and that in the black wall is towards the left. Thus the magnetization in the domain on the right of the figure is downward and that on the left is upward. The point at which the Néel wall changes sense is the intersection of a Bloch line with the surface. With respect to the topology of the magnetic vector field, this point is a magnetic singularity. The magnetization circulates about this point. A component of magnetization must exist perpendicular to the surface. We have been able to detect this perpendicular component of magnetization with the present SEMPA resolution of 40 nm so the range of the singularity can be investigated.

TOWARD HIGHER SPATIAL RESOLUTION

We turn now to the possibility of obtaining higher spatial resolution in the lateral direction. While the present resolution of 40 nm is adequate for many applications, opportunities arise where still higher resolution would be desirable. The investigation of the magnetic singularity just discussed would benefit from higher resolution. As another example, investigation of 100 nm experimental magnetic structures requires a resolution of order 10 nm. Our present SEM with a LaB_6 source is optimum for SEMPA in the range above 100 nm. With a field emission source, which is optimum below 100 nm, we expect to obtain SEMPA images with a spatial resolution better than 10 nm. Note that although there is sufficient incident electron beam current to obtain SEM topography images at a resolution of a couple of nanometers, it is insufficient to obtain SEMPA images in times short enough to avoid other problems such as stage drift.

Achieving spin sensitive imaging at spatial resolutions better than that attainable with a field emission SEM remains a challenge. We have discussed [8] two general approaches: 1) scanned tip microscopy in the field emission mode to achieve a small diameter unpolarized scanned electron beam, and 2) scanning tunneling microscopy where the tip is a source of spin polarized electrons. The ultimate goal is spin sensitive imaging with atomic resolution which would allow investigation of magnetic surface reconstructions and even antiferromagnetic structures.

The most straightforward approach is scanned tip field emission microscopy which was pioneered many years ago by Young et al. [9] for imaging surface topography. Adding spin sensitivity is directly analogous to SEMPA and is illustrated by Fig. 1 with the SEM electron beam replaced by the beam from a scanning field emitter. The apparatus for this is just a scanning tunneling microscope (STM) with the tip pulled back to run in the field emission rather than the tunneling mode. The questions to be

answered are 1) what is the secondary electron yield and can these electrons be extracted to the spin analyzer, and 2) what spatial resolution can be obtained?

The voltage applied to the tip for field emission also has the undesired effect of forcing the low energy secondary electrons back to the sample. We have made calculations for a model tip consisting of a 10 nm radius spherical surface on a 10 degree shank. At a tip to sample spacing of 100 nm and with 30 V on the tip, calculation of electron trajectories show that no secondary electrons are emitted. Only electrons with more than 25 eV energy can escape the tip-to-sample field. Lower energy electrons which are returned to the sample may subsequently escape or generate other secondary electrons, but spatial resolution is then lost. Elastically scattered electrons are expected to have a polarization [10] on the order of 1% and electrons which have lost a couple of eV in scattering from an Fe-based ferromagnetic glass were shown [11] to have a polarization of 5 to 10%. Thus, even in the absence of secondary electrons, it may still be possible to obtain images of magnetic microstructure by energy and spin analysis of the scattered electrons. At the large tip to sample spacing of 1 mm, true secondary electrons can be extracted and their spin polarization measured [12]; the spatial resolution is of course very low.

The resolution of the STM is strongly determined by the details of the tunneling tip. In the field emission mode, the main contribution to the resolution originates from the transverse Fermi velocity of the emitted electrons. The electrons are therefore emitted at room temperature into an approximately 4 degree cone angle. Fink [13] has prepared well characterized single atom tips and measured such a cone angle. This translates into a potential lateral resolution of 7 nm for a 100 nm spacing as in the example above, or, for example, a resolution of 3.5 nm for a tip at a 50 nm spacing and a 20V bias. Such scanned tip microscopy is relatively inexpensive and simple compared to an SEM and can be easily integrated with STM studies. When scanned tip field emission microscopy is developed to the point of obtaining spin sensitive images, it will clearly have many applications.

It may be possible to measure spin configurations on the atomic or at least sub-nanometer scale by exploiting the tunneling of spin polarized electrons. The tunneling current from a ferromagnetic tip is expected to be spin polarized. The spin polarization of electrons field-emitted from Fe is 25% and 20% for tips oriented along the [100] and [111] axes respectively [14]. This is a substantial degree of polarization, especially since the nearly unpolarized s and p electrons are believed to tunnel with 10 to 100 times the probability of the magnetic d electrons. It is important to know the orientation of the spins at the tip and ideally to control this orientation. As the STM scans from one domain to another, the spin dependent part of the signal will change. The difficulty will be in separating a spin dependent signal which is only a few per cent of a topographic signal with large variations. Some form of modulation of the spin dependent signal is clearly necessary. Reversing the magnetization of the tip would be satisfactory if this can be done without otherwise disturbing the STM. Another possibility is spectroscopic modulation [8] in which first the bias and position is set for tunneling to nonmagnetic states and then changed to emphasize tunneling to magnetic states.

There are further complications in a spin sensitive STM employing a magnetic tip to study a magnetic sample. Bringing a tip near to the surface can change the magnetization distribution of the sample and of the tip itself. Our calculations which produced Fig. 6, have been extended to include a magnetic tip near the surface. They show conclusively that a magnetic tip cannot in general be considered to be a nonperturbative probe [15]. The tip and sample must be considered as a combination and extracting information on the magnetic microstructure will not likely be straightforward except in special circumstances. This problem has been

discussed for the case of magnetic force microscopy, where the problems are similar, and optimum conditions suggested [16].

An ideal spin-sensitive STM would consist of an emitter of spin polarized electrons, a means to easily modulate the polarization,and no perturbing interaction between tip and the sample. Conceptually, an optically pumped semiconductor provides such a source. Photoemission from negative electron affinity has been used for many years as a source of spin polarized electrons [17]. Tunneling between the GaAs tip and magnetic sample proceeds directly through the vacuum barrier without the need for any surface treatment to obtain a negative electron affinity as is required for photoemission. The spin polarized electrons are created by photoexcitation to the conduction band with circularly polarized light. The optical selection rules for circularly polarized light produce an electron spin polarization in the conduction band of 50% which can be easily reversed by reversing the helicity of the light.

We have previously discussed tunneling from an optically pumped GaAs tip and analyzed the incident light necessary to achieve a sufficient density of polarized electrons in the conduction band [8]. In brief, we took as a detection limit 10^{18} cm^{-3} electrons based on STM experiments where tunneling from dopant levels at a density of 10^{18} cm^{-3} in p-type GaAs were just detected.[18] With an electron-hole recombination time of order 10^{-9}sec, the steady-state excited-electron densities $2x10^{16}$ $e/(cm^3\ mW)$. This requires 50 mW of light focused into a 10 μm diameter spot to achieve the detectable density. Not only would a such photon flux heat the sample and cause drift problems, but at light fluxes near this value we observed damage in the GaAs tip. In spite of the initial attractiveness of spin polarized tunneling from GaAs tips, there are formidable engineering problems to overcome and the scheme may only be possible if a much improved STM detection sensitivity is obtained.

CONCLUSION

In summary, we have described how spin polarized electrons can be exploited to investigate magnetic microstructure. In SEMPA we have a powerful tool to study magnetic microstructure down to a resolution, ultimately, of order 10 nm. We showed examples of applications to problems of technological importance, where the magnetic properties of thin film recording media and memory elements depend sensitively on the materials preparation. SEMPA provides the possibility to correlate microscopic magnetic properties, such as edge acuity, with macroscopic ones, such as recording noise and allows one to further investigate the dependence of these on growth and other external parameters. Fundamental questions ranging from the ability of a monolayer film to support domains to the nature of a domain wall intersecting the surface can be addressed by SEMPA. The possibility of obtaining higher resolution by using an STM in the scanning field emission mode and measuring the polarization of the scattered electrons was described. The many challenges in measuring surface spin configurations on the atomic scale by spin dependent tunneling were discussed.

ACKNOWLEDGEMENTS

This work was supported in part by the Office of Naval Research.

REFERENCES

[1] G.G. Hembree, J. Unguris, R.J. Celotta, and D.T. Pierce Scanning Microscopy Supplement 1,229(1987).

[2] K. Koike, H. Matsuyama, H. Todokoro, K. Hayakawa, Scanning Microscopy Supplement 1,241(1987).
[3] D.S. Lo, G.H. Cosimini, L.G. Zierhut, R.H. Dean, and M.C. Paul, IEEE Trans. Magnetics MAG-21,1776(1985).
[4] Y. Yafet and E.M. Gyorgy, Phys. Rev. B38,9145(1988).
[5] J.L. Robins, R.J. Celotta, J. Unguris, and D.T. Pierce, Appl. Phys. Lett. 52,1918(1988)
[6] A. Hubert, IEEE Trans. Magnetics, MAG-11,1285(1975).
[7] M.R. Scheinfein, J. Unguris, R.J. Celotta, and D.T. Pierce, to be published.
[8] D.T. Pierce, Phys. Scr. 38,291(1988).
[9] R. Young, J. Ward, and F. Scire, Rev. Sci. Instrum. 43,999(1972).
[10] J. Unguris, D.T. Pierce, and R. J. Celotta, Phys. Rev. B29,1381(1984).
[11] H. Hopster, R. Raue, and R. Clauberg, Phys. Rev. Lett. 53,695(1984).
[12] R. Allenspach and A. Bischof, Appl. Phys. Lett. 54,587(1989).
[13] H.W. Fink,Phys. Scr. 38,260(1988).
[14] M. Landolt, and Y. Yafet, Phys. Rev. Lett. 40,1401(1978).
[15] M.R. Scheinfein, J. Unguris, D.T. Pierce and R.J. Celotta (to be published.)
[16] U. Hartmann, J. Appl. Phys. 64,1561(1988).
[17] D.T. Pierce, R.J. Celotta, G.-C. Wang, W.N. Unertl, A. Galejs, C.E. Kuyatt, and S.R. Mielczarek, Rev. Sci. Instrum. 51,478(1980).
[18] R.M. Feenstra and J.A. Stroscio, J.Vac. Sci. Technnol. B5,923(1987).